Commun Nonlinear Sci Numer Simulat 133 (2024) 107975

Contents lists available at ScienceDirect

Communications in Nonlinear Science and Numerical Simulation

journal homepage: www.elsevier.com/locate/cnsns

Research paper

Symmetry of the stochastic Rayleigh equation and features of bubble dynamics near the Blake threshold

A.O. Maksimov

Pacific Oceanological Institute, Far Eastern Branch of the Russian Academy of Sciences, Baltic Str., 43, Vladivostok, 690041, Russia

ARTICLE INFO

Keywords:
Bubble dynamics
Lie groups
Blake threshold

ABSTRACT

Ultrasonic cleaning is widely accepted as being an extremely efficient method of decontaminating a diverse range of objects and products. Optimization of the process is generally achieved by variation in the intensity and the spectrum of ultrasound. This spectrum takes the form of individual lines, which are superimposed on the noise background. The stochastic dynamics of the bubble in the acoustic field, consisting of a strong harmonic and noise components, is considered. Application of Lie groups reveals the internal symmetry of the problem. An analytical solution of the problem has been derived in the vicinity of the static stability threshold (Blake threshold). A greater understanding of the stochastic bubble dynamics leads to determining the optimal conditions for ultrasonic cleaning.

1. Introduction

The cleaning of a material plays an important role in the production of food, fabrication of electronic devices and the removal of biological materials from an interface. The cleaning process should cause the least possible damage to the substrate. Amongst the many possible methods to achieve these goals, ultrasonic cleaning has been found to be useful [1–3]. Ultrasound technology uses the action of bubbles driven by ultrasonic irradiation of the media to clean an interface and cavitation is certainly a key factor in this mechanism [4].

Once the cavitation is generated, a cavitation bubble may undergo two different kinds of radial oscillations, which are referred as inertial and non-inertial cavitation. The former refers to the situation where the cavitation nuclei (usually microscopic pre-existing gas/vapor bubbles) grow and implode violently within a few cycles of excitation. The collapse being dominated by the inertial forces of the moving liquid rather than the pressure and stiffness of the gas. In contrast, non-inertial cavitation is an oscillation governed by a balance between the liquid inertia and the gas stiffness, such that bubbles can sustain the pulsation and repetitively oscillate for a longer period of time.

The spectrum of the acoustic emission from cavitation field in liquid has the form of single lines rising above a continuum of 'white' noise base [5]. The positions of the lines correspond to harmonics, subharmonics, and ultra-subharmonics of the excitation frequency. The presence of single lines in the spectrum is related to the strongly nonlinear dynamics of gas bubbles. The commonly accepted explanation for the presence of the noise base is the generation of short pulses accompanying the collapse of single inclusions. Individual spectral lines of the cavitation radiation are characterized by a finite width and even by a definite shape.

The theoretical framework is one of the key elements necessary to understand the physical processes accompanying acoustic cavitation. The progress made in the study of bubble dynamic over more than a century is reflected in recent publications [6,7] and reviews [8,9]. Thus, a special section of the Physics of Fluids dedicated to cavitation includes 86 works [10].

E-mail address: maksimov@poi.dvo.ru.

https://doi.org/10.1016/j.cnsns.2024.107975
Received 7 November 2023; Received in revised form 31 January 2024; Accepted 11 March 2024
Available online 15 March 2024
1007-5704/

A study of the sound field generated by cavitation activity is important and the reason for researching this interaction and feedback between the cavitation and the sound field is that ultrasonic cleaning faces technical challenges that have never been overcome, and the root of many of these lies with an understanding of the interaction between the bubble population and the sound field. A special issue of Ultrasonics Sonochemistry (2015;29;519–628) is devoted to the problem of cleaning with bubbles. This paper addresses those features that do exist in the pressure field, but which differ from the idealized field used in traditional modeling.

The bubbles with radii exceeding 10^{-5} m (which are the kind of bubbles we will consider in this paper) are high-Q oscillatory systems that suppress the oscillation spectrum outside a narrow band near the fundamental frequency; i.e., they play the role of bandpass filters. In the main order of magnitude, the bubble is not susceptible to the entire complex spectrum, but to its rather narrow part. In this band, radiation of bubbles, randomly arranged in the cavitation field, is naturally divided into coherent and stochastic components. To indicate the last we will use the term noise.

The effect of fluctuations associated with the random field component is found to be most pronounced in the vicinity of the bifurcation values of the field amplitude [11,12]. These values correspond to changes in the number of stable bubble states. This paper will consider the effect of using a less idealized driving field on the Blake threshold, which predicts the explosive grow of bubbles in the first stage of inertial cavitation, for the limit when the driving sound field is at frequencies much less than the bubble pulsation resonance condition.

Application of Lie groups reveals the internal symmetry of the problem. An analytical solution of the problem has been derived in the vicinity of the static stability threshold (Blake threshold). The behavior of bubbles in these domains is characterized by significantly non-Gaussian distribution of the fluctuations. This is reflected in a very specific change in the shape of the spectral lines of acoustic emission. That, in turn, allows one to diagnose the processes occurring in a cavitation field.

2. The stochastic Rayleigh equation

This section deals with the Rayleigh equation that describes nonlinear oscillations of a gas bubble in an acoustic field [4]

$$\begin{aligned} &R\frac{d^2R}{dt^2}+\frac{3}{2}\left(\frac{dR}{dt}\right)^2-\frac{P_0}{\rho_0}\left(\frac{R_0}{R}\right)^{3\gamma}+\frac{2\sigma}{\rho_0 R}+2\delta R_0\frac{dR}{dt}\\ &=-\left[P_\infty-p_m\cos(\omega_p t)+p_N(t)\right]\rho_0^{-1}, \end{aligned} \tag{1}$$

where R and R_0 are the current end equilibrium radii of the bubble, P_0 is the equilibrium pressure in the bubble, $P_\infty = P_0 - 2\sigma/R_0$ is the external equilibrium pressure, σ is the coefficient of the surface tension, ω_p is the frequency of the external field, γ is the polytropic exponent, δ is the damping coefficient, and ρ_0 is the density of the liquid. The noise component $p_N(t)$ is described by the additional term in the expression for the external field acting on the bubble $P(t) = P_\infty - p_m\cos(\omega_p t) + p_N(t)$.

To make the problem a closed one, it is necessary to describe the characteristics of the random force. We use the most simple force model in the form of a delta-correlated random process $\langle p_N(t+t')p_N(t')\rangle = G_0\delta(t)$, where G_0 is the intensity of the delta correlated process.

The Rayleigh Eq. (1) can be transformed to the dimensionless vector form of the Langevin equation that is the traditional form for analysis of stochastic processes [13].

$$\begin{aligned} &\dot{x}_1 = x_2,\\ &\dot{x}_2 = \frac{1}{x_1}\left[-\frac{3}{2}x_2^2-2\tilde{\delta}x_2+\frac{1}{3\gamma(1+\eta)}\left(\frac{(1+\alpha)}{x_1^{3\gamma}}-\frac{\alpha}{x_1}-u_1\right)\right]-\frac{\tilde{p}_N(t)}{3\gamma(1+\eta)x_1},\\ &\quad x_1=\frac{R}{R_0},\ x_2=\frac{1}{\Omega_0 R_0}\frac{dR}{dt}=\frac{d}{d\tau}\left(\frac{R}{R_0}\right)=\dot{x}_1,\ \tau=\Omega_0 t,\ \tilde{\delta}=\delta/\Omega_0,\\ &\quad \alpha=2\sigma/\left(P_\infty R_0\right),\ \Omega_0^2=\Omega_e^2(1+\eta),\ \Omega_e^2=\left(\frac{3\gamma P_\infty}{\rho_0 R_0^2}\right),\ \tilde{p}_m=p_m/P_\infty,\\ &\quad \tilde{p}_N=p_N/P_\infty,\ \eta=\frac{3\gamma-1}{3\gamma}\alpha,\ u_1=1-\tilde{p}_m\cos\left[(\omega_p/\Omega_0)\tau\right]. \end{aligned} \tag{2}$$

From the rigorous mathematical point of view, these equations cannot be analyzed as a set of differential equations owing to the fast and irregular oscillations of $\tilde{p}_N$, but can be considered as an Ito system [13].

$$dx_i = f_i(\mathbf{x},\tau)d\tau + \sigma_{ik}(\mathbf{x},\tau)dw_k(\tau), \tag{3}$$

where $f_i(\mathbf{x},\tau)$ is the drift vector, $\sigma_{ik}(\mathbf{x},\tau)$ is a nonzero diffusion matrix, and $w_k(\tau)$ are independent homogeneous standard Wiener processes, so that $\langle |w_i(\tau') - w_k(\tau)|^2\rangle = \delta_{ik}\delta(\tau'-\tau)$. Here $\langle\cdots\rangle$ denotes ensemble average. In the case considered here, we have:

$$\begin{aligned} &f_1 = x_2,\ f_2=\frac{1}{x_1}\left[-\frac{3}{2}x_2^2-2\tilde{\delta}x_2+\frac{1}{3\gamma(1+\eta)}\left(\frac{(1+\alpha)}{x_1^{3\gamma}}-\frac{\alpha}{x_1}-u_1\right)\right],\\ &\sigma_{11}=\sigma_{12}=\sigma_{21}=0,\ \sigma_{22}=\frac{\sqrt{G_0\Omega_0}}{3\gamma(1+\eta)P_\infty}\frac{1}{x_1},\ w(\tau)=\sqrt{\frac{\Omega_0}{G_0}}\int_0^t dt'\,p_N(t'). \end{aligned} \tag{4}$$

The general method of the description of the evolution of the system (3) is based on the solution of the Einstein–Fokker–Planck (EFP) equation for the probability density of the dynamical states $W(\mathbf{x},\tau) = \langle \delta(\mathbf{x} - \mathbf{x}(\tau)) \rangle$ [13]. The EFP equation associated with the Ito Eq. (3) has the following form:

$$\partial_\tau W(\mathbf{x},\tau) + \partial_i \left[f_i(\mathbf{x},\tau) W(\mathbf{x},\tau) \right] = \frac{1}{2} \partial^2_{ij} \left[\left(\sigma\sigma^T \right)_{ij} W(\mathbf{x},\tau) \right]. \tag{5}$$

The explicit form of the EFP equation corresponding to (4) is

$$\begin{aligned} &\frac{\partial W(\mathbf{x},\tau)}{\partial \tau} + \frac{\partial}{\partial x_1} \left[x_2 W(\mathbf{x},\tau) \right] + \frac{\partial}{\partial x_2} \left\{ \frac{1}{x_1} \left[-\frac{3}{2} x_2^2 - 2\tilde{\delta} x_2 \right.\right. \\ &\left.\left. + \frac{1}{3\gamma(1+\eta)} \left(\frac{(1+\alpha)}{x_1^{3\gamma}} - \frac{\alpha}{x_1} - u_1 \right) \right] W(\mathbf{x},\tau) \right\} = \frac{D}{x_1^2} \frac{\partial^2 W(\mathbf{x},\tau)}{\partial x_2^2}, \\ &D = \frac{G_0 \Omega_0}{18\gamma^2 (1+\eta)^2 P_\infty^2}. \end{aligned} \tag{6}$$

Eqs. (2) and (6) contain the same statistical information [13].

The presence of a relatively small random perturbation can lead to noticeable effects only near singular dynamic states of the bubble. Solving Eq. (2) with the use of an asymptotic expansion in the small parameter $\epsilon = |R - R_0|/R_0 \ll 1$ allowed us to conduct the analysis in the vicinity of the fundamental resonance, the first and second harmonics, and the first and second subharmonics [11]. These results are correct to third order terms in ϵ. The application of numerical methods in analyzing the nonlinear dynamics of a bubble in the resonance and noise fields has been a natural continuation of this study [12]. Nevertheless, it is desirable to formulate the models which will not be based on perturbation techniques for analyzing this highly nonlinear phenomenon.

3. Symmetry of the stochastic Rayleigh equation

Symmetry methods are by now recognized as one of the tools for solving deterministic differential equations. The application of the theory of continuous groups [14–17] for analyzing the symmetry of equations of bubble dynamics made it possible to obtain new integrals of motion and exact analytical solutions [18,19].

A symmetry group of a system of differential equations $\dot{x}_i = f_i(\mathbf{x},\tau)$ transforms solutions of the system to other solutions, and is the local group of transformations acting on the independent and dependent variables of the system. An important element of Lie group theory and transformation groups is the infinitesimal transformation, by which one can replace the criteria for invariant functions and subsets by an equivalent linear condition of infinitesimal invariance under the corresponding infinitesimal generators of the group action.

For the case of system of first order ODE $\dot{x}_i = f_i(\mathbf{x},\tau)$ the general form of Lie-point vector field (infinitesimal generators) is $\mathbf{X} = \chi(\mathbf{x},\tau)\partial_\tau + \xi_i(\mathbf{x},\tau)\partial_i$ and symmetries of this system are given by $\mathbf{X}$ as above with coefficients satisfying

$$\partial_\tau \left(\xi_i - \chi f_i \right) + \left(f_j \cdot \partial_j \right) \xi_i - \left(\xi_i \cdot \partial_j \right) f_j = 0. \tag{7}$$

For given functions $f_i(\mathbf{x},\tau)$, corresponding to the Rayleigh equation, the partial differential Eqs. (7) have the following solutions [18]:

$$\mathbf{X}_1 = \frac{\partial}{\partial \tau}, \quad \mathbf{X}_2 = \tilde{\tau} \frac{\partial}{\partial \tau} + \frac{2}{2+3\gamma} x_1 \frac{\partial}{\partial x_1} - \frac{3\gamma}{2+3\gamma} x_2 \frac{\partial}{\partial x_2}. \tag{8}$$

The first solution is realized in conditions of steady external pressure ($\partial u_1/\partial \tau = 0$). This group is the group of time translation. Its presence has the result that the Rayleigh equation has an integral of motion i.e. a Hamiltonian that ignores dissipation.

The second group is the group of scaling transformations G_2: $x_1'/x_1 = \lambda^{2/(2+3\gamma)}$, $x_2'/x_1 = \lambda^{-3\gamma/(2+3\gamma)}$. This group is realized when the external field takes the special form $u_1(\tau) = u_0 \left(\tau_0/(\tau_0+\tau) \right)^{6\gamma/(2+3\gamma)}$, $\left(\tilde{\tau} = \tau_0 + \tau \right)$ corresponding to a shock wave with the pressure drop $p_m = u_1(0) P_0$ at the leading edge and with the characteristic fall time $t_0 (\tau_0 \equiv t_0 \Omega_0)$.

The progress achieved in studying the symmetry properties of stochastic differential equations [20–27] allows us to use this approach to analyze the stochastic behavior of a bubble in a cavitation field. In finding the Lie-point symmetry group of the Ito form of the Rayleigh stochastic equation (2), (4) we follow Gaeta [21,23]. It was shown by Gaeta that the vector field $\mathbf{X} = \chi(\mathbf{x},\tau)\partial_\tau + \xi_i(\mathbf{x},\tau)\partial_i$ is a symmetry generator for the Ito equation (3) if and only if the coefficients (χ, ξ_i) satisfy the full deterministic equations

$$\begin{aligned} &\partial_\tau \left(\xi_i - \chi f_i \right) + \left(f_j \cdot \partial_j \right) \xi_i - \left(\xi_i \cdot \partial_j \right) f_j + (1/2) \left(\sigma \cdot \sigma^T \right)_{jk} \partial^2_{jk} \xi_i = 0, \\ &\left(\sigma_{kj} \cdot \partial_j \right) \xi_i - \left(\xi_j \cdot \partial_j \right) \sigma_{ki} - \chi \partial_\tau \sigma_{ki} + (1/2) \sigma_{ik} \partial_\tau \chi = 0. \end{aligned} \tag{9}$$

For given functions $f_i(\mathbf{x},\tau)$, $\sigma_{ik}(\mathbf{x},\tau)$ (4) corresponding to the Rayleigh equation, the partial differential equations (9) have a unique solution, $\mathbf{X}_1 = \partial_\tau$, realized in conditions of steady external pressure ($\partial u_1/\partial \tau = 0$).

It was shown by Gaeta [23] that symmetries of the Ito equation result in the symmetries of the associated EFP equation. Thus we conclude that time translations represent a symmetry group of the EFP equation associated with stochastic Rayleigh equations for the steady external field.

The symmetries of the EFP equation are given by generators of the following form:

$$\mathbf{X} = \chi(\mathbf{x},\tau)\partial_\tau + \xi_i(\mathbf{x},\tau)\partial_i + \phi\partial_W, \text{ with } \phi = A(\mathbf{x},\tau) + B(\mathbf{x},\tau)W. \tag{10}$$

Appealing to linearity gives us "trivial" symmetries $\mathbf{X}_A = A(\mathbf{x},\tau)\partial_W$, with $A(\mathbf{x},\tau)$ an arbitrary solution of the EFP equation itself, this is just expressing the linear superposition principle. Thus, in finding "nontrivial" symmetries we take $A(\mathbf{x},\tau) = 0$. Unfortunately, the EFP equation (6) has no "nontrivial" symmetries except time translations.

The knowledge of the exact symmetries of ordinary differential equations allows us to reduce it, and sometimes to completely solve it. However, in many cases one would be satisfied with an approximate rather than exact solution. It turns out, that in this case, situations of approximate symmetry are as good as exact ones.

4. Bubble dynamics in quasi-static field

The time translation symmetry is absent for periodic driving. Nevertheless such symmetry can be restored for special cases, for example, when the driving period is long compared to the time scale of the bubble's eigenoscillations ($\epsilon_p \equiv (\omega_p/\Omega_0) \ll 1$). Thus, we can consider the regular part of the external pressure as quasi-static. In this case, in the leading order in the small parameter ϵ_p, inertial terms and damping in Eq. (4) can be neglected [28]. Then Rayleigh equation in the absence of noise reduces to

$$\frac{(1+\alpha)}{x_1^3} - \frac{\alpha}{x_1} = u_1(\tau) = 1 - \tilde{p}_m \cos T,\ T = \omega_p t = \epsilon_p \tau, \tag{11}$$

where the isothermal law was used for the gas ($\gamma \approx 1$), which is certainly a good approximation for the static situation.

For $u_1(\tau) > 0$, Eq. (11) has exactly one solution and it corresponds to a stable equilibrium.

$$\begin{aligned} x_1^0(T) = &-\frac{\alpha}{3(1-\tilde{p}_m\cos T)} + \left\{ -\frac{\alpha^3}{3^3\left(1-\tilde{p}_m\cos T\right)^3} + \frac{(1+\alpha)}{2\left(1-\tilde{p}_m\cos T\right)} \right. \\ &\left. \times\left[1+\sqrt{1-\frac{4\alpha^3}{3^3(1+\alpha)\left(1-\tilde{p}_m\cos T\right)^2}}\right]\right\}^{1/3} + \left\{ -\frac{\alpha^3}{3^3\left(1-\tilde{p}_m\cos T\right)^3} \right. \\ &\left. + \frac{(1+\alpha)}{2\left(1-\tilde{p}_m\cos T\right)}\left[1-\sqrt{1-\frac{4\alpha^3}{3^3(1+\alpha)\left(1-\tilde{p}_m\cos T\right)^2}}\right]\right\}^{1/3}. \end{aligned} \tag{12}$$

If $u_1(\tau) < 0$ but is small in absolute magnitude, two equilibria exist, the one at larger radius being unstable. The pressure in the liquid at the bubble wall oscillates at a value given by the static pressure (hydrostatic plus atmospheric pressures) plus the applied oscillatory pressure. When the amplitude of oscillation of the applied pressure exceeds the static pressure, the liquid momentarily goes into tension, but this is not enough to cause explosive bubble growth because of the restraining effect of surface tension. The amplitude of oscillation of the applied pressure must be increased further (attaining the Blake threshold pressure) to overcome this surface tension effect (such that $u_1^B < 0$ and the two equilibria points merge), causing explosive bubble growth for a short time. Increases in the acoustic amplitude beyond the Blake threshold pressure will extend this time during which growth occurs (and the two equilibria points that merged on achieving the Blake threshold have now disappeared). Such explosive growth is the first (but not the only) criterion for inertial cavitation to occur. Obviously, the most sensitive point in the cycle is $\tau = 0$ where $u_1(0) = (1-\tilde{p}_m)$ is negative and of magnitude $\tilde{p}_m - 1$. The smaller the bubble, the stronger the surface tension forces that resist growth, and therefore a larger acoustic pressure is needed to cause explosive bubble growth. The Blake threshold condition therefore depends on two parameters: the acoustic pressure and the initial bubble radius. That is to say, for a given $\tilde{p}_m$ there is a critical $R_0 = R_0^{tr}$ above which the two positive real solutions of (11) become complex. The transient ambient radius R_0^{tr} at given $\tilde{p}_m$ is obtained [28] as

$$\begin{aligned} R_0^{tr} = \frac{2\sigma}{3P_\infty}&\left\{\left[\frac{2}{(\tilde{p}_m-1)^2} - 1 + \frac{2}{(\tilde{p}_m-1)}\left(\frac{1}{(\tilde{p}_m-1)^2}-1\right)^{1/2}\right]^{1/3}\right. \\ &\left.+\left[\frac{2}{(\tilde{p}_m-1)^2} - 1 + \frac{2}{(\tilde{p}_m-1)}\left(\frac{1}{(\tilde{p}_m-1)^2}-1\right)^{1/2}\right]^{-1/3} - 1\right\}. \end{aligned} \tag{13}$$

When R_0 exceeds R_0^{tr}, there is a period of time around $\tau = 0$ where the right hand side of (11) cannot be zero, but must be positive. Then, the dynamical terms that have been neglected so far must become noticeable and a dynamical expansion follows which can only be stopped when $u_1(\tau)$ has again become large enough to allow a stable radius equilibrium. The critical radius corresponds to the maximum value of the acoustic pressure amplitude at which a bubble can exist in an equilibrium state, the Blake threshold.

Below the Blake's threshold ($R_0 \ll R_0^{tr}$), our results are based on an asymptotic analysis for the stochastic Rayleigh equation in a weak noise approximation [13]

$$dx_i = f_i(\mathbf{x},\tau)d\tau + \epsilon_N \sigma_{ik}(\mathbf{x},\tau)dw_k(\tau), \tag{14}$$

where ϵ_N is a small parameter. Perturbation theory leads to an expression for the desired solution in terms of a formal power series in this parameter

$$x_1(\tau) = x_1^0(T) + \epsilon_N x_1^1(\tau,T) + \epsilon_N^2 x_1^2(\tau,T) + \cdots$$

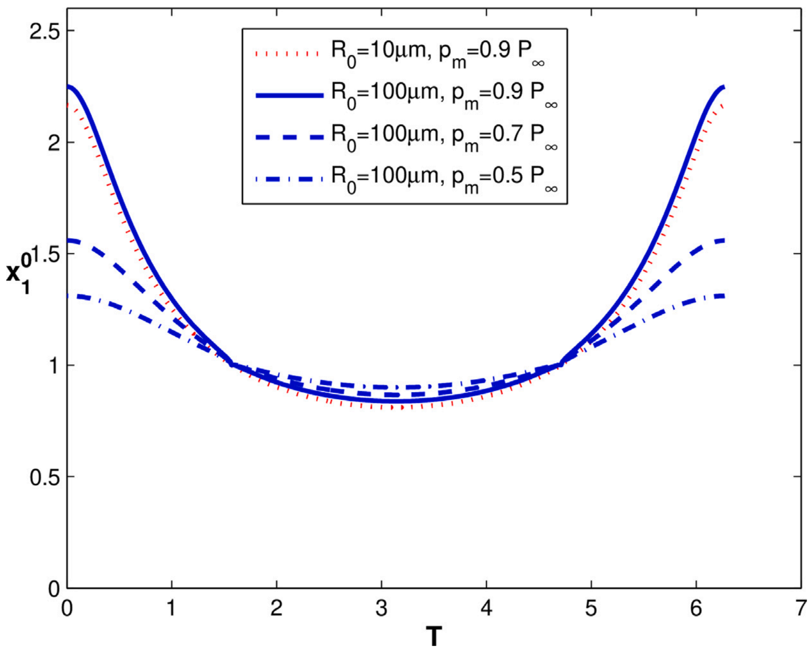

Fig. 1. Variation of the quasi-static dimensionless bubble radius x_1^0 over the period of the external force T : $[0.2\pi]$. The solid, dashed, and dash-dotted lines correspond to $\tilde{p}_m = 0.9$, 0.7, 0.5. The calculations have been performed for the following values of the parameters: $\sigma = 72$ mN/m, $P_\infty = 10^5$ Pa, $R_0 = 100$ μm. For comparison, the dotted line corresponds to $\tilde{p}_m = 0.9$, $R_0 = 10$ μm.

$$x_2(\tau) = \epsilon_N x_2^1(\tau, T) + \epsilon_N^2 x_2^2(\tau, T) + \cdots . \tag{15}$$

where $x_1^0(T)$ is determined by quasi-static solution (12).

The investigations of general bubble behavior in a cavitation plume produced by an operating ultrasonic horn [29] and bubble swarms which aid the cleaning of an interface [30–32] deal with the characteristic bubble sizes of the first hundred of micrometers. For water of surface tension $\sigma = 72$ mN/m, equilibrium pressure $P_\infty = 10^5$ Pa and the bubbles of radius $R_0 = 100$ μm, the parameter α is small $\alpha \approx 0.015$. Fig. 1 illustrates the form of the quasi-static solution x_1^0 for a set of the pressure amplitudes: $\tilde{p}_m = 0.5, 0.7, 0.9$. For comparison, the dotted line shows the variation of a relatively small bubbles $R_0 = 10$ μm for the pressure amplitude $\tilde{p}_m = 0.9$. These sizes are characteristic for filamentary bubble structures [33–35]. The difference between the variations of x_1^0 for lower pressure amplitudes (at greater distances from the threshold) is insignificant, and therefore not shown in the figure. At time moments $T = \pi/2, 3\pi/2$, the driving force vanishes ($p_m \cos T = 0$), and the bubble is in the initial, equilibrium state $x_1^0 = 1$. With the increase of the field amplitude and approaching the threshold, the instability begins to manifest itself at a stage of the bubble expansion.

The equation of the first order in this chain describes a time-dependent Ornstein–Uhlenbeck process [13]. In the considered case we have

$$\begin{aligned} dx_1^1 &= x_2^1 d\tau, \\ dx_2^1 &= \frac{1}{x_1^0(T)}\left[-2\tilde{\delta} x_2^1 - \frac{x_1^1}{\left(x_1^0(T)\right)^4}\right] d\tau + \frac{\sqrt{G_0 \Omega_0}}{3 P_\infty x_1^0(T)} dw, \end{aligned} \tag{16}$$

where we ignored small corrections $(1+\eta) \approx 1$, $\gamma \approx 1$.

When dealing with the linear stochastic equation, it is convenient to introduce the Green's function, which is expressed through solutions of a homogeneous equation. In our case, a homogeneous equation describes an oscillator whose parameters varying slowly over time (compared to the natural frequency). The corresponding solution obtained by the multiscale method is well known and leads to the following result:

$$\begin{aligned} x_1^1(\tau) = &\int_0^\tau d\theta \exp\left(-\tilde{\delta}\int_\theta^\tau \frac{d\tau'}{x_1^0(\epsilon_p \tau')}\right) \sin\left(\int_\theta^\tau \frac{d\tau'}{\left[x_1^0(\epsilon_p \tau')\right]^{5/2}}\right) \\ &\times \left[x_1^0(\epsilon_p \tau) x_1^0(\epsilon_p \theta)\right]^{5/4} \frac{\tilde{p}_N(\theta)}{x_1^0(\epsilon_p \theta)}. \end{aligned} \tag{17}$$

Table 1
The spectral composition of the quasistatic solution x_1^0 for a set of the pressure amplitudes.

	a_1	a_2	a_3	a_4	a_5	a_6	a_7
$R_0 = 100$ μm, $\tilde{p}_m = 0.9$	0.513	0.216	0.110	0.057	0.035	0.019	0.015
$R_0 = 100$ μm, $\tilde{p}_m = 0.7$	0.299	0.081	0.030	0.010	0.008	0.0024	0.005
$R_0 = 100$ μm, $\tilde{p}_m = 0.5$	0.188	0.033	0.011	0.002	0.005	0.0008	0.004
$R_0 = 10$ μm, $\tilde{p}_m = 0.9$	0.431	0.163	0.077	0.036	0.022	0.011	0.010

Thus the bubble response is the sum of coherent $x_1^0(T)$ and random $x_1^1(\tau, T)$ components non-linearly depending on the driving amplitude $\tilde{p}_m$. The variance of the stochastic component has the following form

$$
\begin{aligned}
Var\left(x_1^1\right) &\equiv \left\langle x_1^1(\tau)x_1^1(\tau)\right\rangle = \frac{G_0\Omega_0}{12P_\infty^2}\int_0^\tau d\theta \exp\left(-2\tilde{\delta}\int_\theta^\tau \frac{d\tau'}{x_1^0(\epsilon_p\tau')}\right) \\
&\times \sin^2\left(\int_\theta^\tau \frac{d\tau'}{\left[x_1^0(\epsilon_p\tau')\right]^{5/2}}\right)\left[x_1^0(\epsilon_p\tau)\right]^{5/2}\left[x_1^0(\epsilon_p\theta)\right]^{1/2} \approx \frac{G_0\Omega_0^2}{36\delta P_\infty^2}\left(x_1^0(T)\right)^4 \\
&\times\left[1 - \frac{\left[\delta/x_1^0(T)\right]^2}{\left[\Omega_0/(x_1^0(T))^{5/2}\right]^2 + \left[\delta/x_1^0(T)\right]^2}\right] \approx \frac{G_0\Omega_0}{36P_\infty^2}\left(\frac{\Omega_0}{\delta}\right)\left(x_1^0(T)\right)^4 .
\end{aligned} \tag{18}
$$

The resonance and proximity to the Blake threshold are the two key factors that lead to the substantial value of the stochastic component in bubble oscillations. The appearance of the quality factor $Q \propto \Omega_0/\delta$ in Eq. (18) is the result of resonance. A significant growth of the factor $\left(x_1^0(T)\right)^4$ at the moments $T = 2\pi n$ $(n = 0, 1, 2, \ldots)$ is due to the proximity to the Blake threshold.

5. Spectral density

The power spectral density of the bubble oscillations is determined by the expression

$$
\begin{aligned}
S(\omega) &= \frac{1}{2\pi}\int_{-\infty}^{+\infty} ds e^{-\mathrm{i}\omega s}\lim_{T_L\to\infty}\frac{1}{T_L}\int_0^{T_L} dt\left[x_1^0(\omega_p t) + x_1^1(t)\right] \\
&\times\left[x_1^0(\omega_p(t+s)) + x_1^1(t+s)\right] .
\end{aligned} \tag{19}
$$

This spectrum is formed by the correlations of two different types: the auto-correlation function of the quasi-static oscillations and the auto-correlation function of the stochastic component. Thus we naturally separate the coherent and incoherent contributions to the spectral density. Note that we assume ergodicity of the system in calculating the spectral function of the noise component.

The coherent part of the spectral function is obtained as

$$
\begin{aligned}
S_c(\omega) &= \sum_{n=1}^{\infty}\frac{a_n^2}{4}\left[\delta(\omega - n\omega_p) + \delta(\omega + n\omega_p)\right] , \\
a_n &= \frac{2}{\pi}\int_0^\pi dT x_0(T)\cos(nT) = \frac{2}{\pi}\int_0^\pi dT\frac{(1+\alpha)^{-1/3}\cos(nT)}{\left(1 - \tilde{p}_m\cos T + \frac{\alpha}{x_0(T)}\right)^{1/3}},
\end{aligned} \tag{20}
$$

where we have dropped the term with $n = 0$ which is insignificant for the study of dynamic effects.

Table 1 illustrates the spectral composition of the quasistatic solution x_1^0 for a set of the pressure amplitudes: $\tilde{p}_m = 0.9, 0.7, 0.5$ (series 1, 2, 3). Calculations have been performed for the following values of the parameters: $\sigma = 72$ mN/m, $P_\infty = 10^5$ Pa, $R_0 = 100$ μm. Series (4) shows the difference in spectral composition with decreasing bubble size. In this case, the calculations are performed for $R_0 = 10$ μm, $\tilde{p}_m = 0.9$.

The autocorrelation function of the stochastic component has the following form

$$
\begin{aligned}
S_{st}(\omega, T) &= \frac{1}{\pi}\int_0^\infty ds\cos(\omega s)\left\langle x_1^1(t)x_1^1(t+s)\right\rangle \\
&= \frac{G_0\Omega_0}{36P_\infty^2}\frac{1}{\pi}\int_0^\infty ds\cos(\omega s)\left[\frac{x_1^0(\omega_p(t+s))}{x_1^0(\omega_p t)}\right]^{5/4}\exp\left(-\delta\int_t^{t+s}\frac{dt'}{x_1^0(\omega_p t')}\right) \\
&\times\left\{\frac{\Omega_0}{\delta}\left[x_1^0(\omega_p t)\right]^4\cos\left(\Omega_0\int_t^{t+s}\frac{dt'}{\left[x_1^0(\omega_p t')\right]^{5/2}}\right) + \left[x_1^0(\omega_p t)\right]^{11/2}\right. \\
&\times\left.\sin\left(\Omega_0\int_t^{t+s}\frac{dt'}{\left[x_1^0(\omega_p t)\right]^{5/2}}\right)\right\} \approx \frac{G_0}{36P_\infty^2}\left[x_1^0(T)\right]^3
\end{aligned}
$$

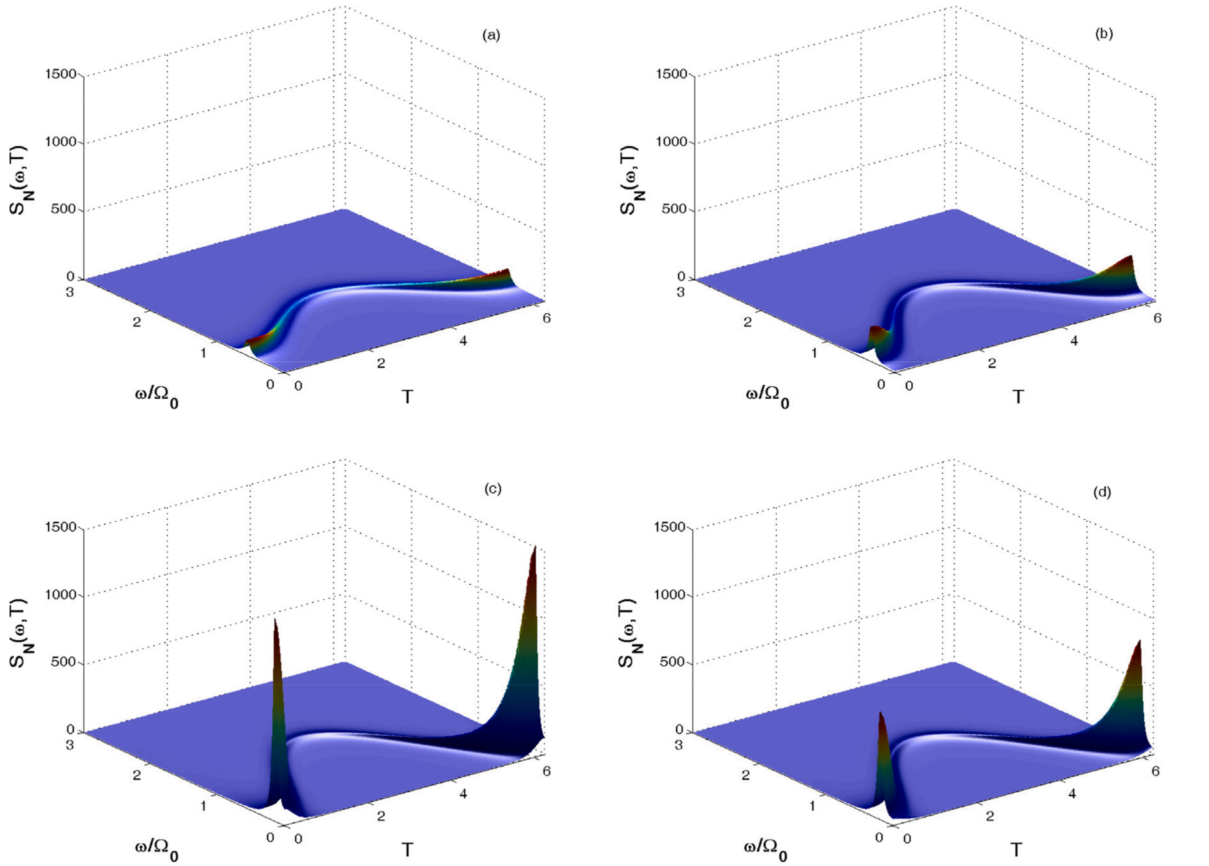

Fig. 2. Normalized spectral density of stochastic component of bubble oscillations, S_N, as a function of the dimensionless frequency ω/Ω_0 and slow time $T=\omega_p t$. Panels (*a*), (*b*), (*c*) show the results of calculations for $R_0 = 100$ μm, $\tilde{p}_m = 0.5, 0.7, 0.9$. The last panel (*d*) corresponds to $R_0 = 10$ μm, $\tilde{p}_m = 0.9$.

$$\times\frac{1}{\pi}\frac{\omega^2/\Omega_0^2+\left[x_1^0(T)\right]^{-5}}{\left[\omega^2/\Omega_0^2-\left[x_1^0(T)\right]^{-5}\right]^2+2\frac{\delta^2}{\Omega_0^2}\left[x_1^0(T)\right]^{-2}\left[\omega^2/\Omega_0^2+\left[x_1^0(T)\right]^{-5}\right]}. \tag{21}$$

The integrand in Eq. (21) contains a factor with a rapidly oscillating phase (with a frequency Ω_0). When calculating the integral over s, we took advantage of the fact that the oscillating phase does not have stationary points. For this reason, the asymptotic expansion is carried out by integration by parts and the main contribution comes from the neighborhood of $s = 0$.

The behavior of the incoherent correlation function is determined by the resonance of an oscillator, parameters of which (natural frequency, damping and coupling) are slowly varying in time with the period of the driving field.

The surfaces in Fig. 2 show graphs of the normalized spectral density $S_N = S_{st}(\omega,T)\times\left(36P_\infty^2/G_0\right)$ versus dimensionless frequency ω/Ω_0 and slow time $T=\omega_p t$. The first three panels (*a*), (*b*), (*c*) correspond to a bubble with radius of 100 μm driven by a sound field with a dimensionless pressure amplitude $\tilde{p}_m = 0.5, 0.7, 0.9$. The panel (*d*) describes the spectral density of the bubble with a smaller radius of 10 μm driven by a sound field $\tilde{p}_m = 0.9$.

In carrying out the calculations, we used the following model for the damping coefficient entering into Eq. (21). The contribution of the thermal damping δ_{th} is dominant in the total damping factor δ for these conditions and presumed high frequency noise driving. Moreover, since the thermal penetration length $l=\sqrt{D/\omega}$ ($D = 2\cdot 10^{-5}$ m^2 s^{-1} is the thermal diffusivity of air) is much smaller than the radius of the bubble, the following simple formula can be used for the damping coefficient [36]:

$$\delta_{th}=\frac{P_0}{2\rho\omega R^2}\frac{9\gamma(\gamma-1)}{R}\sqrt{\frac{D}{2\omega}}. \tag{22}$$

The quasi-static bubble radius $R = R_0 x_1^0(T)$ should be used in this formula. Since during evaluation of the spectral density (21) the small damping should be considered only near $\omega/\Omega_0 \approx \left[x_1^0(t)\right]^{-5/2}$, we replaced ω by this value in Eq. (22). Thus, when plotted, we used the following expression for the damping coefficient $\delta_{th} = \delta_{th}(R_0)\left[x_1^0(T)\right]^{3/4}$, where $\delta_{th}(R_0)$ is the thermal damping of the bubble with radius R_0 at resonance.

The proximity to the threshold of instability and a resonance are mechanisms by which a system embedded in a noisy environment acquires an enhanced sensitivity towards small external forcing. As such it highlights the possibility that noise, a phenomenon considered traditionally to constitute a nuisance, may actually play a constructive role.

6. Discussion

A step has been taken in describing cavitation activity and the structure of the sound field. The dynamics of a single inclusion have been described, but there are many bubbles in the cavitation zone that effectively interact with each other due to monopole oscillations associated with changes in their volume. The monopole interaction is long-range in nature, so the bubble is affected by some self-consistent field, which varies on scales exceeding the average distance between bubbles. Approximation of this effective field by a simple model made it possible to describe the dynamics of a single bubble.

The acoustic cavitation spectrum offers a convenient and concise method for presenting cavitation data during an acoustic exposure. However, to describe the observed physical characteristics, it is necessary to find out the details of the formation of a self-consistent field generated by the emission of individual inclusions. Attempts have been made to describe a contribution to the cavitation noise spectrum from periodic shock waves [37], which arise when individual bubbles collapse.

A comparison of the spectral density characterizing the emission of a single bubble with the experimentally recorded acoustic cavitation spectrum is presented in Supplementary materials. Realizing the limitations of the comparison, it was not included in the main text of the article.

The used model of spherically symmetric nonlinear bubble oscillations, described by the Rayleigh equation, has a number of limitations [28,38]. The most obvious of them are associated with the appearance of deformation distortion and patterns formation on the bubble wall [39–41]. Identification of the features of parametric instability of the shape oscillations in the presence of external noise can be achieved using an approach similar to that used in this work.

7. Conclusion

Lie group analysis provides a systematic account of symmetries inherent to the problem of the nonlinear dynamics of a bubble in the field of a harmonic signal in the presence of a random component. The approximate time translation symmetry is restored when the driving period is long compared to the time scale of the bubble's eigenoscillations, which provides an analytical solution of the problem near the Blake threshold.

CRediT authorship contribution statement

A.O. Maksimov: Conceptualization, Data curation, Formal analysis, Funding acquisition, Investigation, Methodology, Project administration, Resources, Software, Validation, Visualization, Writing – original draft, Writing – review & editing.

Declaration of competing interest

The authors declare that they have no known competing financial interests or personal relationships that could have appeared to influence the work reported in this paper.

Data availability

No data was used for the research described in the article.

Acknowledgments

The work was supported by POI FEBRAS, project no. 121021700341-2.

Appendix A. Supplementary data

Supplementary material related to this article can be found online at https://doi.org/10.1016/j.cnsns.2024.107975.

References

[1] Nikitenko SI, Venault L, Pflieger R, Chave T, Bisel I, Moisy P. Potential applications of sonochemistry in spent nuclear fuel reprocessing: a short review. Ultrason Sonochem 2010;17:1033–40. http://dx.doi.org/10.1016/j.ultsonch.2009.11.012.
[2] Seymour IJ, Burfoot D, Smith RL, Cox LA, Lockwood A. Ultrasound decontamination of minimally processed fruits and vegetables. J Food Sci Technol 2002;37:547–57. http://dx.doi.org/10.1046/j.1365-2621.2002.00613.x.
[3] Kumar A, Bhatt RB, Behere PG, Afzal M. Ultrasonic decontamination of prototype fast breeder reactor fuel pins. Ultrasonics 2014;54:1052–6. http://dx.doi.org/10.1016/j.ultras.2013.12.008.
[4] Leighton TG. The acoustic bubble. New York: NY: Academic Press; 1994.
[5] Lauterborn W, Cramer E. On the dynamics of acoustic cavitation noise spectra. Acustica 1981;49:280–7.
[6] Yasui K. Acoustic cavitation and bubble dynamics. Springer briefs in molecular science ultrasound and sonochemistry, Cham: Springer Nature; 2018.
[7] A-Man Zhang, Shi-Min Li, Pu Cui, Shuai Li, Yun-Long Liu. A unified theory for bubble dynamics. Phys Fluids 2023;35:033323.
[8] Pengfei Wu, Xiuming Wang, Weijun Lin, Lixin Bai. Acoustic characterization of cavitation intensity: A review. Ultrason Sonochem 2022;82:105878.
[9] Folden TS, Aschmoneit FJ. A classification and review of cavitation models with an emphasis on physical aspects of cavitation. Phys Fluids 2023;35:081301.
[10] Khoo BC, Giacomin AJ, Hatzikiriakos SC, Feigl KA, Phan-Thien N. Special issue on flow cavitation. Phys Fluids 2023;36:110401.
[11] Maksimov AO. Spectrum of acoustic radiation caused by cavitation: Analytical model. Acoust Phys 2001;47:93–101.
[12] Maksimov AO, Sosedko EV. Peculiarities of the nonlinear dynamics of a gas bubble under the action of resonance and noise acoustic fields. Tech Phys Lett 2003;29:102–4.
[13] Gardiner CW. Handbook of stochastic methods for physics, chemistry, and the natural sciences. Berlin: Springer; 1986.
[14] Olver PJ. Application of Lie groups to differential equations. New York: NY: Springer; 1993.
[15] Ibragimov NH. Elementary Lie group analysis and ordinary differential equations. Chichester: John Wiley & Sons; 1999.
[16] Ibragimov NH, Meleshko SV. Invariants and invariant description of second-order ODEs with three infinitesimal symmetries II. Commun Nonlinear Sci Numer Simul 2008;13:1015–20.
[17] Ibragimov NH, Ibragimov RN. Invariant solutions as internal singularities of nonlinear differential equations and their use for qualitative analysis of implicit and numerical solutions. Commun Nonlinear Sci Numer Simul 2009;14:3537–47.
[18] Maksimov AO. Symmetry of the Rayleigh equation and the analysis of nonlinear gas bubble oscillations in liquid. Acoust Phys 2002;48:713–9.
[19] Maksimov AO. Symmetry in bubble dynamics. Commun Nonlinear Sci Numer Simul 2004;9:83–92.
[20] Cicogna G, Gaeta G. Symmetry and perturbation theory in nonlinear dynamics. Berlin: Springer; 1999.
[21] Gaeta G, Quintero NR. Lie-point symmetries and stochastic differential equations. J Phys A: Math Gen 1999;32:8485–505.
[22] Unal G. Symmetries of ito and stratonovich dynamical systems and their conserved quantities. Nonlinear Dynam 2003;32:417–26.
[23] Gaeta G. Symmetry of stochastic equations. Proc Nat Acad Sci Ukraine 2004;50:98–109.
[24] Unal G, Sun JQ. Symmetries and conserved quantities of stochastic dynamical control systems. Nonlinear Dynam 2004;36:107–22.
[25] Ibragimov NH, Jogreus C, Unal G. Approximate symmetries and conservation laws for ito and stratonovich dynamical systems. J Math Anal Appl 2004;297:152–68.
[26] Srihirun B, Meleshko SV, Schulz E. On the definition of an admitted Lie group for stochastic differential equations. Commun Nonlinear Sci Numer Simul 2007;12:1379–89.
[27] Kozlov R. On symmetries of stochastic differential equations. Commun Nonlinear Sci Numer Simul 2012;17(2012):4947–51.
[28] Hilgenfeldt S, Brenner M, Grossmann S, Lohse D. Analysis of Rayleigh-Plesset dynamics for sonoluminescing bubbles. J Fluid Mech 1998;365:171–204.
[29] Birkin PR, Offin DG, Vian CJB, Leighton TG, Maksimov AO. Investigation of noninertial cavitation produced by an ultrasonic horn. J Acoust Soc Am 2011;130:3297–308.
[30] Offin DG, Birkin PR, Leighton TG. An electrochemical and high-speed imaging study of micropore decontamination by acoustic bubble entrapment. Phys Chem Chem Phys 2014;16:4982–9.
[31] Birkin PR, Offin DG, Vian CJB, Leighton TG. Electrochemical bubble swarm enhancement of ultrasonic surface cleaning. Phys Chem Chem Phys 2015;17:21709–15.
[32] Birkin PR, Offin DG, Leighton TG. An activated fluid stream – new techniques for cold water cleaning. Ultrason Sonochem 2016;29:612–8.
[33] Mettin R, Luther S, Ohl C-D, Lauterborn W. Acoustic cavitation structures and simulations by a particle model. Ultrason Sonochem 1999;6:23–30.
[34] Luther S, Mettin R, Koch P, Lauterborn W. Observation of acoustic cavitation bubbles at 2250 frames per second. Ultrason Sonochem 2001;8:159–62. http://dx.doi.org/10.1016/S1350-4177(01)00073-6.
[35] Moussatov A, Granger C, Dubus B. Cone-like bubble formation in ultrasonic cavitation field. Ultrason Sonochem 2003;10:191–5.
[36] Prosperetti A. The thermal behavior of oscillating gas bubbles. J Fluid Mech 1991;222:587–616.
[37] Song JH, Johansen K, Prentice P. An analysis of the acoustic cavitation noise spectrum: The role of periodic shock waves. J Acoust Soc Am 2016;140:2494–505.
[38] Brenner MP, Hilgenfeldt S, Lohse D. Single-bubble sonoluminescence. Rev Modern Phys 2002;74:425–84.
[39] Trinh E, Thiessen D, Holt R. Driven and freely decaying nonlinear shape oscillations of drops and bubbles immersed in a liquid: experimental results. J Fluid Mech 1998;364:253–72.
[40] Versluis M, Goertz DE, Palanchon P, Heitman IL, Meer SMvander, Dollet B, Jong Nde, Lohse D. Microbubble shape oscillations excited through ultrasonic parametric driving. Phys Rev E 2010;82:026321.
[41] Maksimov AO, Leighton TG. Pattern formation on the surface of a bubble driven by an acoustic field. Proc R Soc A. 2012;468:57–75.